U. S. Department of Energy – National Energy Technology Laboratory (NETL)
2023 Virtual Workshop on Multiphase Flow Science – Morgantown-WV-USA – August 1-2, 2023

Effects of particle Froude number on the sub-grid behavior of fluidized gas-particle flows

Chris C. Milioli, Fernando E. Milioli
University of São Paulo - Brazil

At the 2021 NETL Multiphase Flow Science workshop we presented:

On the effect of particle Froude number in sub-grid modeling of gas-solid fluidized flows

Among the conclusions of that work we stated that:

Before new sub-grid models could be derived accounting for particle Froude number, further work would be required to account for:

higher domain average gas Reynolds numbers

a variety of domain average solid volume fractions

Those goals have been achieved, and related outcomes are now exposed in two presentations:

1) Results accounting for ranges of domain average gas Reynolds numbers and solid volume fractions, for a range of particle Froude numbers
2) New sub-grid models for effective drag, filtered and residual stresses

Presentation (1) follows next.

Filtered two-fluid modeling

We ultimately aim to provide sub-grid models for filtered two-fluid modeling.

$$\frac{\partial}{\partial t}\left(\rho_g \bar{\phi}_g\right) + \nabla\cdot\left(\rho_g \bar{\phi}_g \tilde{\boldsymbol{v}}_g\right) = 0 \qquad \frac{\partial}{\partial t}\left(\rho_s \bar{\phi}_s\right) + \nabla\cdot\left(\rho_s \bar{\phi}_s \tilde{\boldsymbol{v}}_s\right) = 0$$

$$\frac{\partial}{\partial t}\left(\rho_g \bar{\phi}_g \tilde{\boldsymbol{v}}_g\right) + \nabla\cdot\left(\rho_g \bar{\phi}_g \tilde{\boldsymbol{v}}_g \tilde{\boldsymbol{v}}_g\right) = -\bar{\phi}_g \nabla\cdot\tilde{\boldsymbol{\sigma}}_g - \nabla\cdot\boldsymbol{\tau}'_g - \bar{\boldsymbol{M}}_I + \rho_g \bar{\phi}_g \boldsymbol{g}$$

$$\frac{\partial}{\partial t}\left(\rho_s \bar{\phi}_s \tilde{\boldsymbol{v}}_s\right) + \nabla\cdot\left(\rho_s \bar{\phi}_s \tilde{\boldsymbol{v}}_s \tilde{\boldsymbol{v}}_s\right) = -\nabla\cdot\bar{\boldsymbol{\sigma}}_s - \nabla\cdot\boldsymbol{\tau}'_s - \bar{\phi}_s \nabla\cdot\tilde{\boldsymbol{\sigma}}_g + \boldsymbol{B}'_{gs} + \bar{\boldsymbol{M}}_I + \rho_s \bar{\phi}_s \boldsymbol{g}$$

$$\bar{\boldsymbol{M}}_I = (1-H)\bar{\beta}\left(\tilde{\boldsymbol{v}}_g - \tilde{\boldsymbol{v}}_s\right)$$

$$\tilde{\boldsymbol{\sigma}}_g = \left[\tilde{P}_g - \left(\lambda_g + \tfrac{2}{3}\mu_g\right)\left(\nabla\cdot\tilde{\boldsymbol{v}}_g\right)\right]\boldsymbol{I} - 2\mu_g \tilde{\boldsymbol{S}}_g$$

$$\bar{\boldsymbol{\sigma}}_s = \left[\bar{P}_s - \overline{\left(\lambda_s + \tfrac{2}{3}\mu_s\right)\left(\nabla\cdot\boldsymbol{v}_s\right)}\right]\boldsymbol{I} - 2\bar{\mu}_s \tilde{\boldsymbol{S}}_s = P_{fil,s}\boldsymbol{I} - 2\mu_{fil,s}\tilde{\boldsymbol{S}}_s$$

$$\boldsymbol{\tau}'_\ell = \rho_\ell \bar{\phi}_\ell \widetilde{\boldsymbol{v}_\ell \boldsymbol{v}_\ell} - \rho_\ell \bar{\phi}_\ell \tilde{\boldsymbol{v}}_\ell \tilde{\boldsymbol{v}}_\ell = P_{res,\ell}\boldsymbol{I} - 2\mu_{res,\ell}\tilde{\boldsymbol{S}}_\ell$$

$$\tilde{\boldsymbol{S}}_\ell = \tfrac{1}{2}\left[\nabla\tilde{\boldsymbol{v}}_\ell + \left(\nabla\tilde{\boldsymbol{v}}_\ell\right)^T\right] - \tfrac{1}{3}\left(\nabla\cdot\tilde{\boldsymbol{v}}_\ell\right)\boldsymbol{I}$$

Effective, filtered and residual closures

$$H = 1 - \frac{\beta_{eff}}{\bar{\beta}} \qquad \beta_{eff} = \frac{\overline{\beta\left(\boldsymbol{v}_g - \boldsymbol{v}_s\right)}}{\left(\tilde{\boldsymbol{v}}_g - \tilde{\boldsymbol{v}}_s\right)}$$

$$P_{fil,s} = \tfrac{1}{3}\mathrm{tr}\left[\bar{P}_s - \overline{\left(\lambda_s + \tfrac{2}{3}\mu_s\right)\left(\nabla\cdot\boldsymbol{v}_s\right)}\right]$$

$$\mu_{fil,s} = \bar{\mu}_s$$

$$P_{res,\ell} = \tfrac{1}{3}\mathrm{tr}\left(\boldsymbol{\tau}'_\ell\right)$$

$$\mu_{res,\ell} = \frac{\left|\boldsymbol{\tau}'_{shear,\ell}\right|}{2\left|\tilde{\boldsymbol{S}}_{shear,\ell}\right|}$$

We go for effective, filtered and residual parameters by filtering over predictions from highly resolved simulations (HRS) with microscopic two-fluid modeling.

Microscopic two-fluid modeling

On the basis of Anderson and Jackson' formulation, with microscopic closures as implemented into the MFIX code by Agrawal et al. (2001).

$$\frac{\partial}{\partial t}\left(\rho_g \phi_g\right) + \nabla\cdot\left(\rho_g \phi_g \boldsymbol{v}_g\right) = 0$$

$$\frac{\partial}{\partial t}\left(\rho_s \phi_s\right) + \nabla\cdot\left(\rho_s \phi_s \boldsymbol{v}_s\right) = 0$$

$$\frac{\partial}{\partial t}\left(\rho_g \phi_g \boldsymbol{v}_g\right) + \nabla\cdot\left(\rho_g \phi_g \boldsymbol{v}_g \boldsymbol{v}_g\right) = -\phi_g \nabla\cdot\boldsymbol{\sigma}_g - \boldsymbol{M}_I + \rho_g \phi_g \boldsymbol{g}$$

$$\frac{\partial}{\partial t}\left(\rho_s \phi_s \boldsymbol{v}_s\right) + \nabla\cdot\left(\rho_s \phi_s \boldsymbol{v}_s \boldsymbol{v}_s\right) = -\nabla\cdot\boldsymbol{\sigma}_s - \phi_s \nabla\cdot\boldsymbol{\sigma}_g + \boldsymbol{M}_I + \rho_s \phi_s \boldsymbol{g}$$

$$\boldsymbol{M}_I = \beta\left(\boldsymbol{v}_g - \boldsymbol{v}_s\right)$$

$$\boldsymbol{\sigma}_\ell = \left[P_\ell - \left(\lambda_\ell + \tfrac{2}{3}\mu_\ell\right)\left(\nabla\cdot\boldsymbol{v}_\ell\right)\right]\boldsymbol{I} - 2\mu_\ell \boldsymbol{s}_\ell$$

$$\boldsymbol{s}_\ell = \tfrac{1}{2}\left[\nabla\boldsymbol{v}_\ell + \left(\nabla\boldsymbol{v}_\ell\right)^T\right] - \tfrac{1}{3}\left(\nabla\cdot\boldsymbol{v}_\ell\right)\boldsymbol{I}$$

Microscopic closures

Drag

Wen and Yu (1966)

Solid phase pressure and viscous stresses

Lun et al. (1984),
as adapted by Agrawal et al. (2001)

Highly resolved simulations (MFIX) / filtering

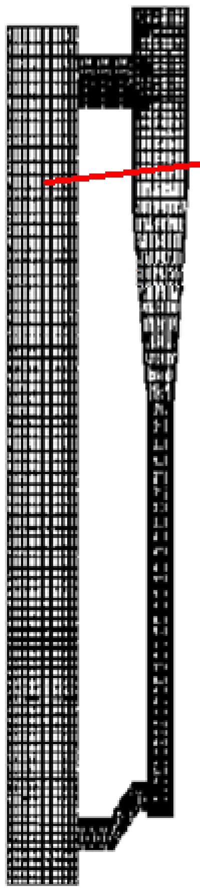

LSS

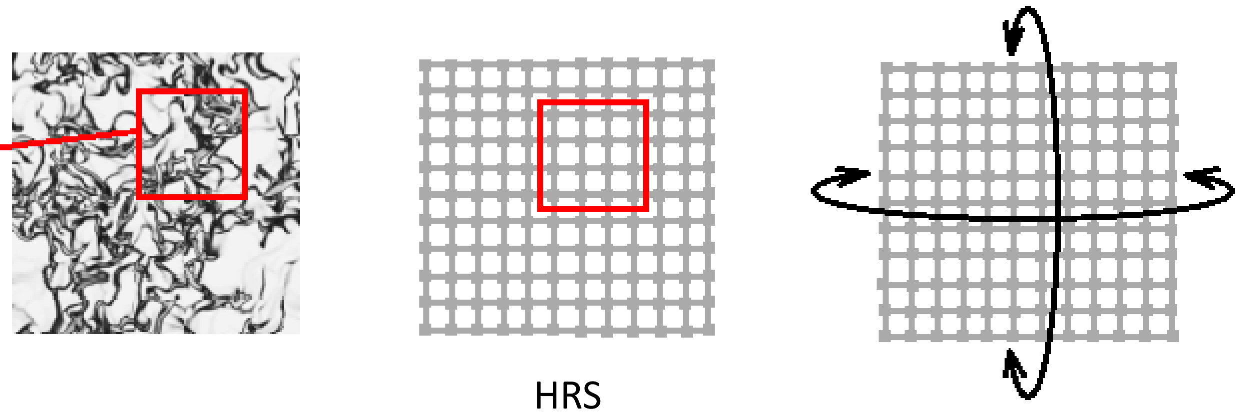

HRS

- All periodic boundaries
- 16 x 16 cm domain
- 128 x 128 grids
- 1.25 x 1.25 mm grid cells
- up to 4 x 4 cm filter sizes

d_p	40 / 75 / 150 / 300 μm
$Fr_p = v_t^2/(g d_p)$	12.21 / 64.85 / 286.69 / 799.22
ρ_s	1500 kg/m^3
e	0.9
ρ_g	1.3 kg/m^3
μ_g	1.8×10^{-5} kg/(m s)
$\langle\phi_s\rangle$	0.05 / 0.15 / 0.25 / 0.35 / 0.45 / 0.55
$\langle Re_g\rangle / \langle Re_g\rangle_{susp}$	1 / 8.15 / 16.30 / 24.45

Filtered data classified by narrow ranges of

$\bar{\phi}_s$, $\tilde{v}_{slip,y}$

Some results

Grayscale plots (in the statistical steady state regime)

For a case with $\langle \phi_s \rangle$ = 0.15 and $\langle \mathrm{Re}_g \rangle / \langle \mathrm{Re}_g \rangle_{susp}$ = 1

[ϕ_s from 0 (white) to 0.64 (black)

$|v_{g,y}/v_{t75}|$ from 0 (white) to >28.71 (black)

$|(v_{g,y} - v_{s,y})/v_{t75}|$ from 0 (white) to >2.93 (black)]

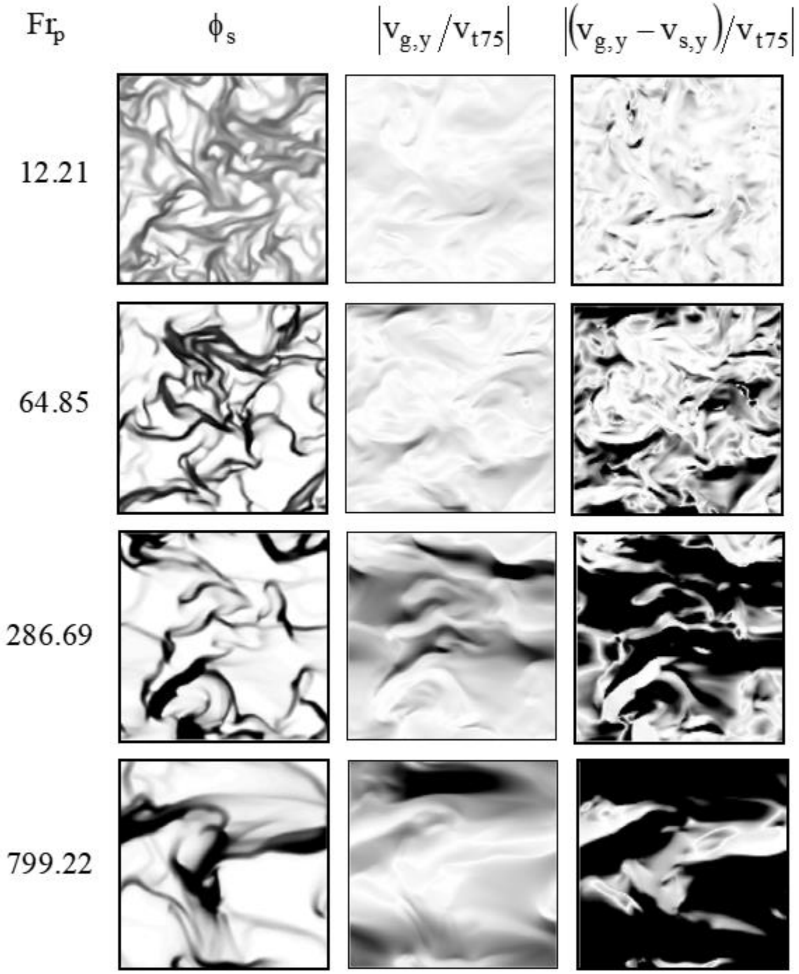

$$\tilde{v}^*_{slip,y} = \left|\tilde{v}_{slip,y} / v_{t75}\right|$$

$$\Delta^*_f = \Delta_f / \left(v^2_{t75} / g\right)$$

$$Fr_p = v^2_t / \left(g d_p\right)$$

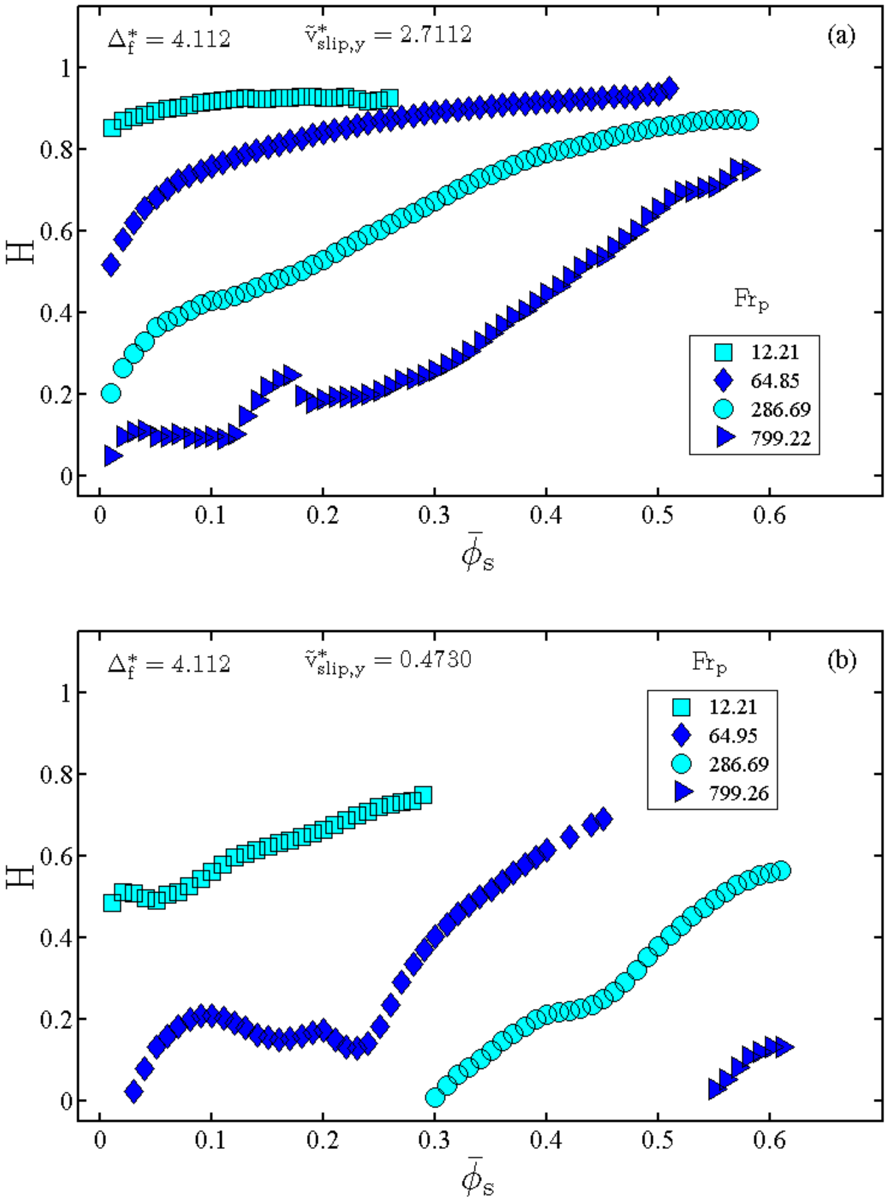

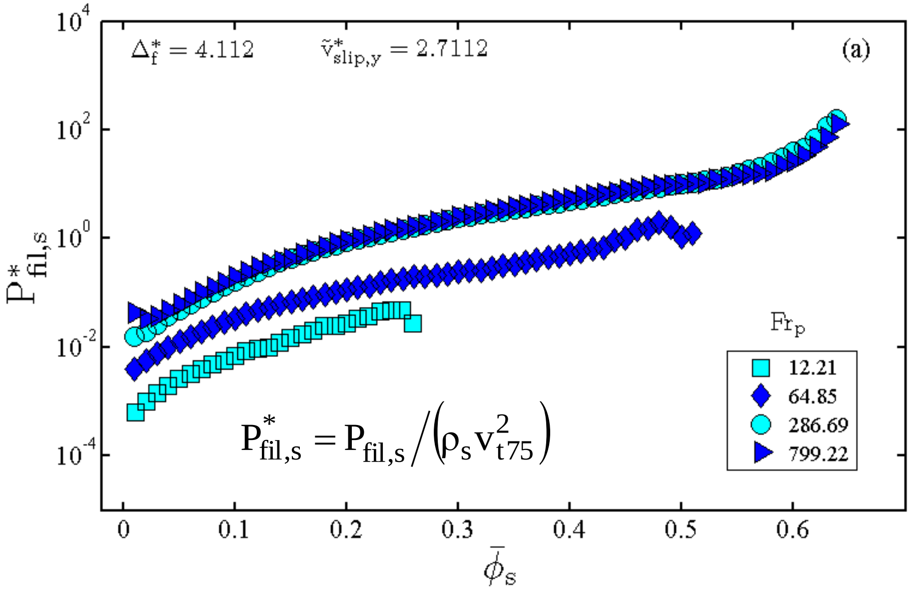
$\Delta_f^* = 4.112$
$\tilde{v}^*_{slip,y} = 2.7112$
(a)
$P^*_{fil,s}$
$P^*_{fil,s} = P_{fil,s} / \left(\rho_s v_{t75}^2\right)$
Fr_p
12.21
64.85
286.69
799.22
$\bar{\phi}_s$

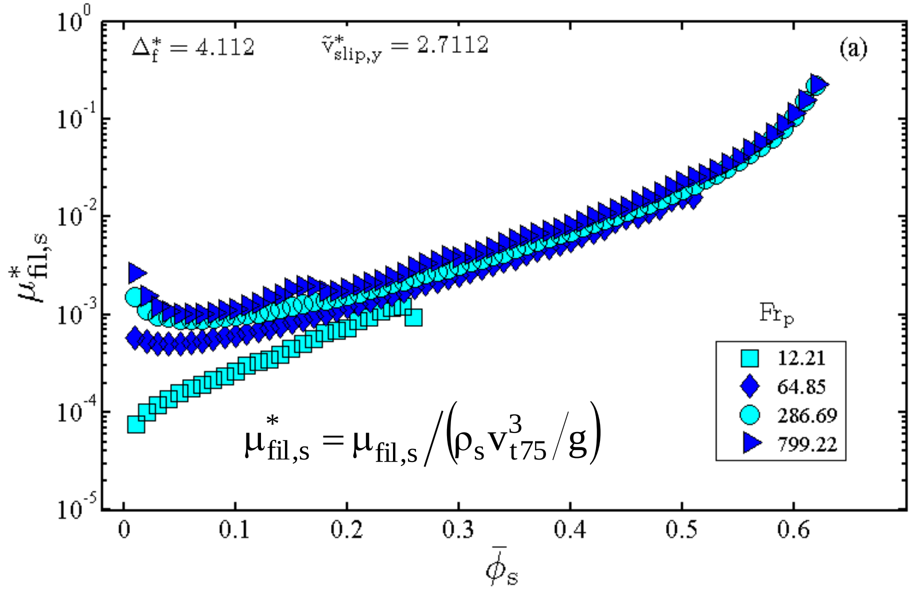
$\Delta_f^* = 4.112$
$\tilde{v}^*_{slip,y} = 2.7112$
(a)
$\mu^*_{fil,s}$
$\mu^*_{fil,s} = \mu_{fil,s} / \left(\rho_s v_{t75}^3 / g\right)$
Fr_p
12.21
64.85
286.69
799.22
$\bar{\phi}_s$

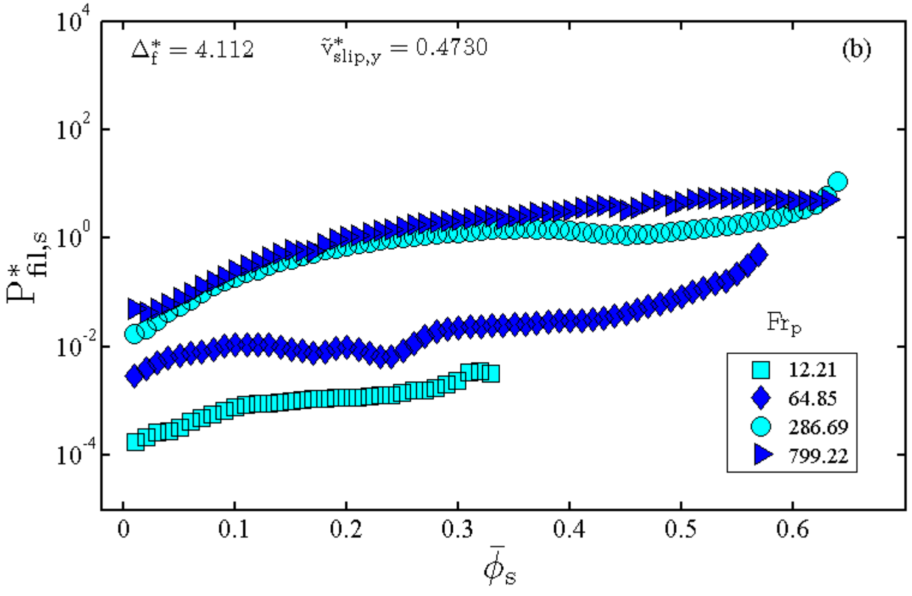
$\Delta_f^* = 4.112$
$\tilde{v}^*_{slip,y} = 0.4730$
(b)
$P^*_{fil,s}$
Fr_p
12.21
64.85
286.69
799.22
$\bar{\phi}_s$

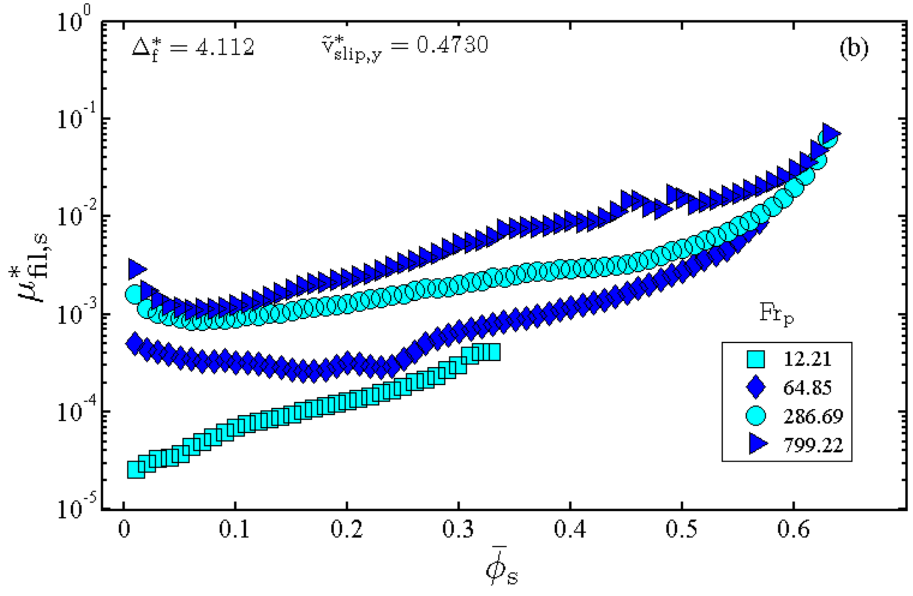
$\Delta_f^* = 4.112$
$\tilde{v}^*_{slip,y} = 0.4730$
(b)
$\mu^*_{fil,s}$
Fr_p
12.21
64.85
286.69
799.22
$\bar{\phi}_s$

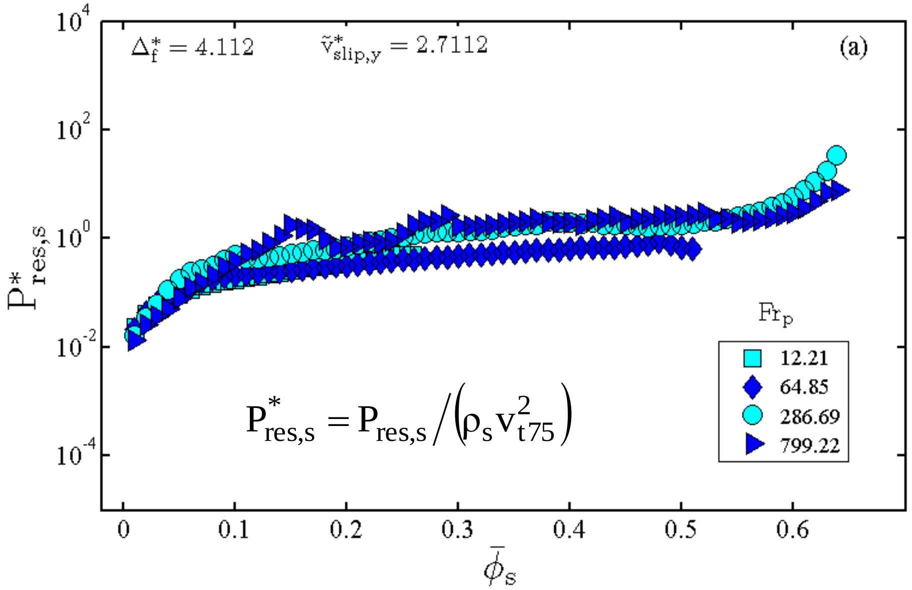

$\Delta_f^* = 4.112$
$\tilde{v}^*_{slip,y} = 2.7112$
(a)
$P^*_{res,s}$
$P^*_{res,s} = P_{res,s}/(\rho_s v_{t75}^2)$
Fr_p
12.21
64.85
286.69
799.22
$\bar{\phi}_s$

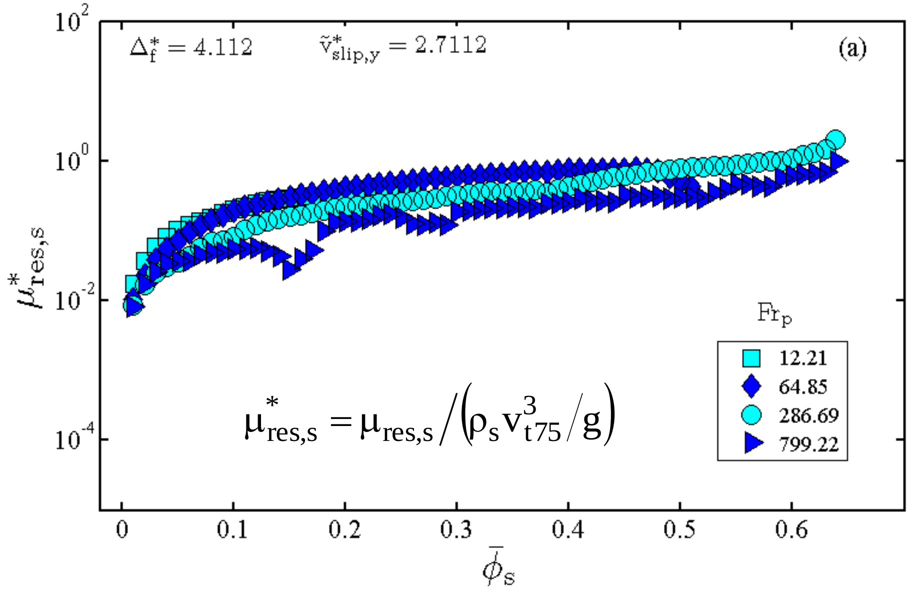

$\Delta_f^* = 4.112$
$\tilde{v}^*_{slip,y} = 2.7112$
(a)
$\mu^*_{res,s}$
$\mu^*_{res,s} = \mu_{res,s}/(\rho_s v_{t75}^3/g)$
Fr_p
12.21
64.85
286.69
799.22
$\bar{\phi}_s$

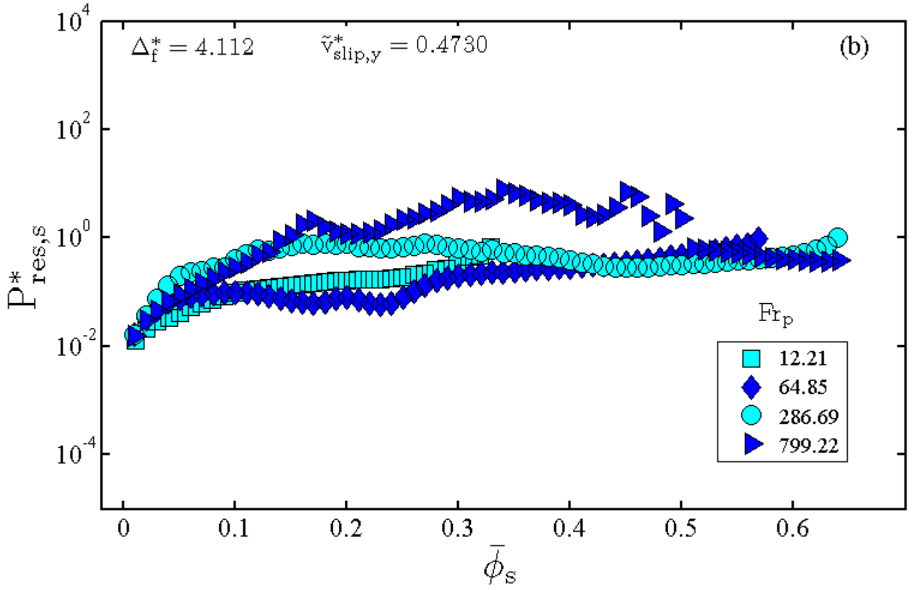

$\Delta_f^* = 4.112$
$\tilde{v}^*_{slip,y} = 0.4730$
(b)
$P^*_{res,s}$
Fr_p
12.21
64.85
286.69
799.22
$\bar{\phi}_s$

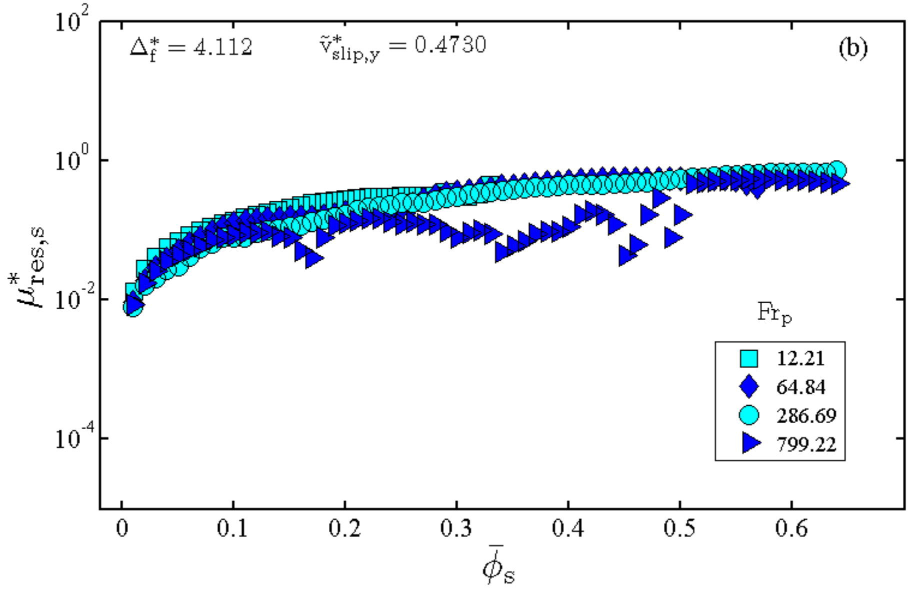

$\Delta_f^* = 4.112$
$\tilde{v}^*_{slip,y} = 0.4730$
(b)
$\mu^*_{res,s}$
Fr_p
12.21
64.84
286.69
799.22
$\bar{\phi}_s$

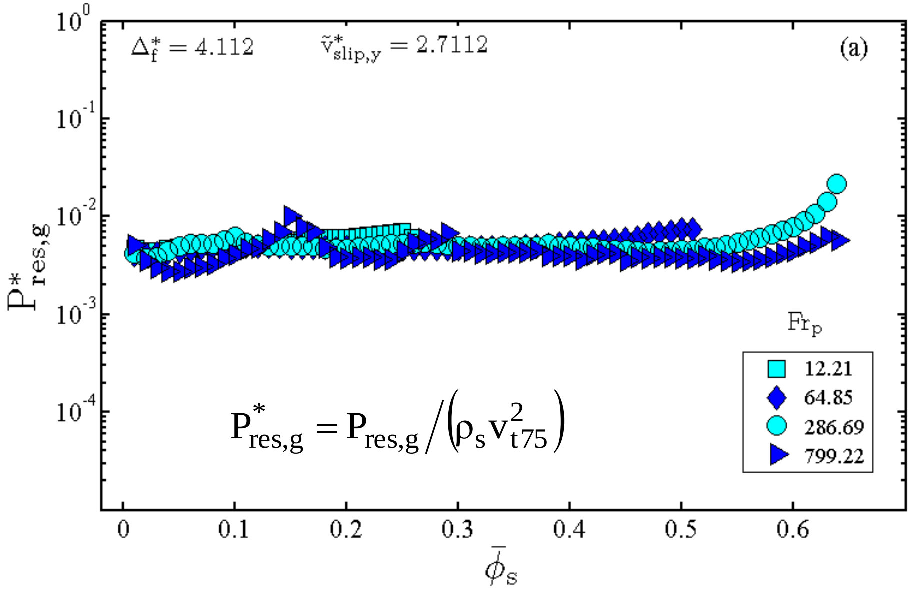
$\Delta_f^* = 4.112$
$\tilde{v}^*_{slip,y} = 2.7112$
(a)
$P^*_{res,g}$
$\bar{\phi}_s$
Fr_p
12.21
64.85
286.69
799.22
$P^*_{res,g} = P_{res,g} / \left(\rho_s v_{t75}^2\right)$

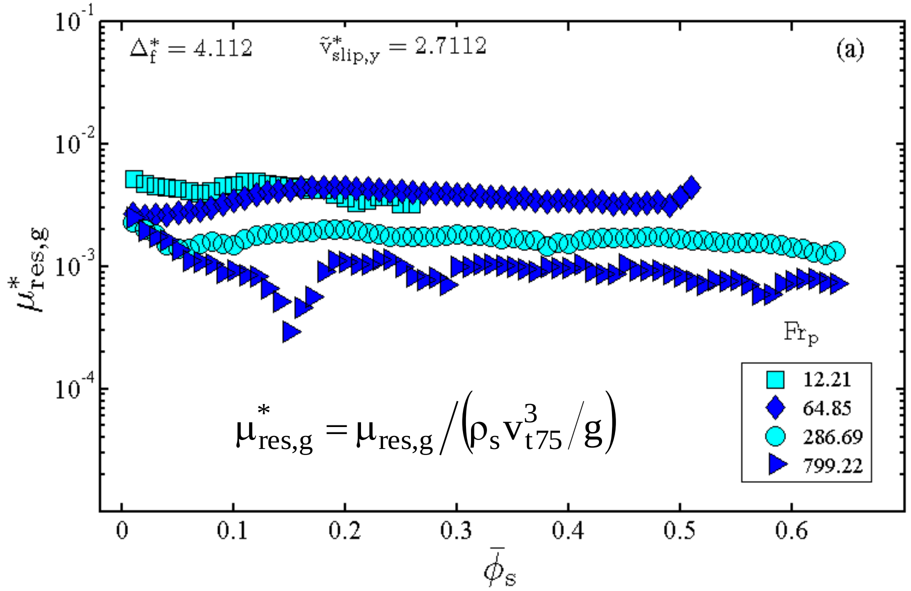
$\Delta_f^* = 4.112$
$\tilde{v}^*_{slip,y} = 2.7112$
(a)
$\mu^*_{res,g}$
$\bar{\phi}_s$
Fr_p
12.21
64.85
286.69
799.22
$\mu^*_{res,g} = \mu_{res,g} / \left(\rho_s v_{t75}^3 / g\right)$

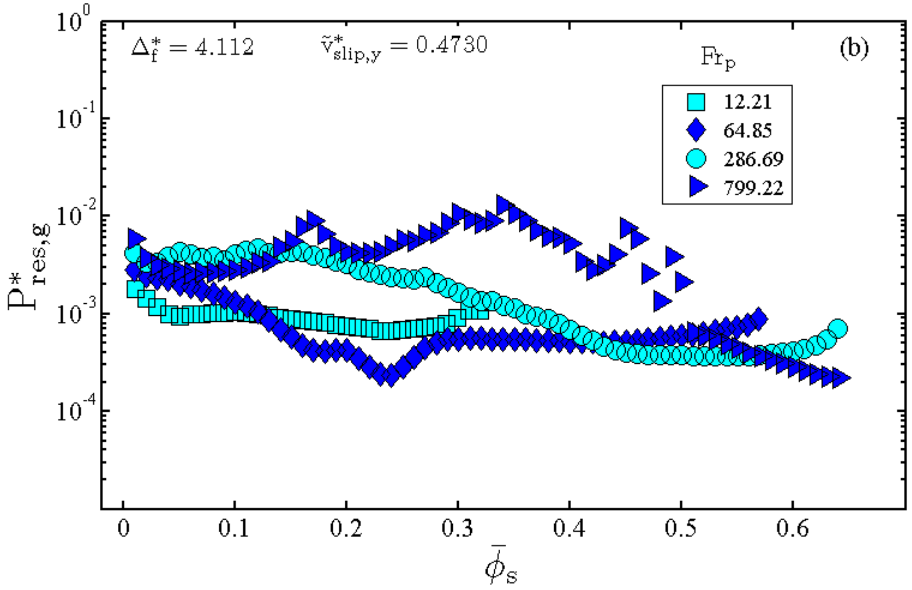
$\Delta_f^* = 4.112$
$\tilde{v}^*_{slip,y} = 0.4730$
(b)
$P^*_{res,g}$
$\bar{\phi}_s$
Fr_p
12.21
64.85
286.69
799.22

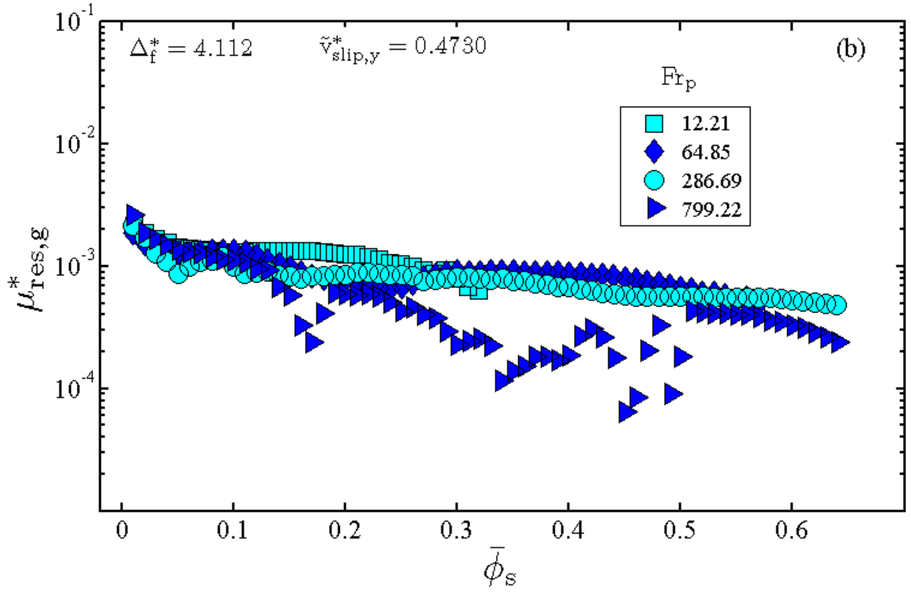
$\Delta_f^* = 4.112$
$\tilde{v}^*_{slip,y} = 0.4730$
(b)
$\mu^*_{res,g}$
$\bar{\phi}_s$
Fr_p
12.21
64.85
286.69
799.22

Conclusions

- Flow heterogeneity grows with decreasing $\mathrm{Fr_p}$ (more refined structures; higher local velocity fluctuations)

  Causing

  - Higher H (higher corrections over homogeneous drag)
  - Higher $\mu^*_{res,s}$, $\mu^*_{res,g}$ (velocity fluctuations/kinetic effects overcome collisional effects)
  - Lower $P^*_{fil,s}$, $\mu^*_{fil,s}$, $P^*_{res,s}$, $P^*_{res,g}$ (collisional effects overcome velocity fluctuations/kinetic effects)

- As compared to the previous study, the present results show similar qualitative behaviors for all the concerning sub-grid parameters, while quantitative differences were observed in response to dissimilar non-local effects caused by the variety of macro-scale conditions that were practiced.

(refer to companion presentation for proposed sub-grid models)

Acknowledgements

This work was supported by

CNPq FAPESP

Please direct any questions to milioli@sc.usp.br

Thank you very much!